Large-scale Thematic Mapping of Volcanic Domes in Armenia Based on Ultra-high Resolution Data

Anastasia Ponomareva [1], Andrey Medvedev [2,3]

[1] Faculty of Geography and Geoinformation Technology, Higher School of Economics, Moscow, Russia – aiponomareva_2@edu.hse.ru

[2] Institute of Geography, Russian Academy of Sciences, Moscow, Russia – medvedev@igras.ru

[3] Center for Ecological-Noosphere Studies National Academy of Sciences, RA, Yerevan, Armenia - andrey.medvedev@cens.am

Keywords: Photogrammetry, UAV, Volcanic Domes of Armenia, Large-Scale Mapping, GIS, Geomorphology

Abstract: The volcanic domes of Armenia hold significant value as both natural heritage and vital research sites for the study of volcanic activity and geomorphological processes. However, detailed geological mapping of these formations has only been conducted at scales of 1:100,000 and 1:200,000. The use of UAVs and high-resolution satellite imagery (Sentinel-2, Resurs-P, PlanetScope) offers new opportunities for large-scale mapping and monitoring of these geological features. This study focuses on the Ajdahak, Armagan, Eratumber, and Arailer volcanoes located in the Gegham Highlands and their surrounding areas. These volcanoes, which include cinder cones and a stratovolcano, showcase a variety of geological structures such as lava flows, barrancos, and erosion formations. Multispectral and thermal UAV surveys were conducted using Mavic Pro, Mavic 3M, and Mavic 3T drones equipped with RTK (Real Time Kinematic) positioning systems, as well as optical, multispectral, and thermal sensors. The collected data was processed through photogrammetry to generate dense point clouds, digital surface models (DSMs), and thermal and multi-channel orthophotos. Morphometric analysis and spectral indices (NDVI, SAVI, GSAVI, etc.) enabled the classification of vegetation, soil cover, and volcanic rock types. The resulting thematic maps provide high-resolution representations of landforms, land cover, and anthropogenic transformations, which are crucial for understanding geodynamic changes, predicting hazards, supporting land-use planning, and preserving Armenia's volcanic heritage. Based on the results of the study, an improved method of automated relief analysis using UAV imagery and derived ultra-high resolution DEM/DSM data, as well as their integration with multispectral imagery data, was developed for thematic mapping of volcanic domes.

1. INTRODUCTION

Modern remote sensing methods are increasingly used to study geological and geomorphological objects, including volcanic formations. These technologies provide high-precision data on the composition of rocks, landform features, and landscape dynamics, offering numerous opportunities for mapping and monitoring natural processes. This research applied technologies for remote analysis, including multispectral and thermal imaging. Data obtained using unmanned aerial vehicles (UAVs) and satellite systems were also utilized.

One of the research methods involved multispectral imaging, which allows for geological and geomorphological mapping. The analysis of spectral characteristics enables the determination of the mineralogical composition of rocks (Van Ruitenbeek et al., 2012); for a detailed analysis of the morphometric features of volcanic formations, data from UAVs were used. UAVs provide high-precision digital terrain models and orthomosaic (Westoby et al., 2012). Combining UAV data with satellite imagery has been applied to monitor volcanic activity, such as Montserrat Island (James et al., 2017), demonstrating its effectiveness in identifying morphological changes and surface deformations. Furthermore, thermal imaging detected temperature anomalies indicating volcanic activity or geothermal processes (Harris et al., 2005). Spectral indices such as NDVI and SAVI were employed to assess environmental changes and dynamics in vegetation and soil cover, among others. These indices allow for the analysis of biophysical parameters of vegetation as well as the detection of changes in soil cover (Bannari et al., 1995). Combining field observations with laboratory analyses enabled obtaining detailed information about physical properties like ash's impact on its surroundings (Durán et al., 2020).

Multispectral imaging is widely applied in geology and geomorphology to analyze geological structures, types of rocks, soil conditions, and landscape forms. Each rock mineral possesses unique spectral characteristics depending on its chemical composition and physical properties. Cameron & Kumar 2018 These characteristics determine electromagnetic radiation reflection absorption levels at various wavelengths, allowing differentiation of materials on Earth's surface. Collected data was analyzed by comparing measured spectral profiles and reference profiles of minerals stored in specialized databases. This classifies materials and maps spatial distribution Gewali et al.; Spectral differences can indicate weathering hydrothermal alterations moisture content erosion degree.

Satellite remote sensing is widely used for studying geology and geomorphology and monitoring volcanic activity. Data from satellites such as MODIS, NOAA, and Sentinel are applied to detect thermal anomalies and track the spread of ash clouds (Coppola et al., 2016). Multispectral and hyperspectral imaging allow for a detailed analysis of the spectral characteristics of rocks and minerals. Research by Van der Meer et al. (2014) demonstrated the effectiveness of these methods for mapping different types of volcanic rocks and identifying hydrothermally altered zones. LiDAR helps create highly detailed digital surface models (DSMs) of volcanic areas. The work by Favalli et al. (2009) shows that LiDAR data can be used to analyze the morphology of lava flows and estimate the volume of erupted material. SAR is used to detect deformations on volcano surfaces. Studies by Pinel et al. (2014) showed how this method allows for identifying minor changes in volcano structure that may precede eruptions.

This study aims to create highly detailed thematic maps of volcanoes Ajdaak, Armagan, Eratumber, and Arailer using multispectral and thermal imaging from UAVs combined with data from Sentinel-2, Resurs-P, and PlanetScope satellites. The main research question focuses on how integrating data from various platforms and sensors enhances the accuracy and informativeness of mapping volcanic domes while revealing features related to their geological structure and dynamics in geomorphological processes.

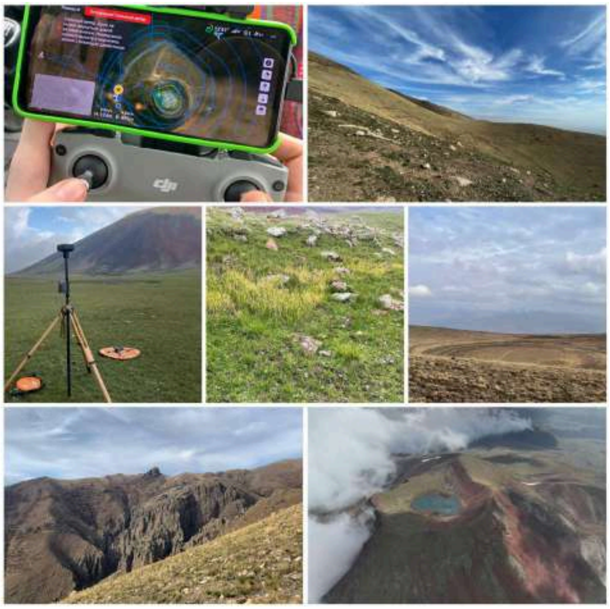

Figure 1. Conducting fieldworks.

2. METHODOLOGY

2.1. Study area

The volcanic domes of Armenia are natural monuments that reflect the country's geological and geomorphological features. The objects of study—volcanoes Ajdaak, Armagan, Eratumber, and Arailer—are typical examples of volcanoes in Armenia (Svyatlovsky, 1959; Aslanyan, 1958). Despite their significance, detailed geological mapping of these objects has been limited to scales of 1:100 000 and 1:200 000 (Karapetyan et al., 1973).

Volcano Arailer (Karnyarikh) is located between the Araqats massif and the Gegham Highlands on the northern slope of the Yerevan depression between the rivers Kasakh and Razdan (Svyatlovsky, 1959). It is a dormant Quaternary stratovolcano with a height of approximately 2614 meters. The base perimeter is about 85 km, and the crater diameter is about two kilometers (Asatrian,1999).

Volcanoes Armagan, Eratumber, and Ajdaak are situated within the Gegham Highlands. Significant landform changes occurred here during the Neogene-Quaternary period (Karapetyan et al.,1973). All three volcanoes are composed primarily of late Quaternary basaltic to basalt-andesitic lavas (Aslanyan1968) and belong to central-type volcanoes with scoria cones. Volcano Armagan has a symmetrical cone; barrancos dissect its southern slope while lava flows solidify on its northwestern slope, reaching Lake Sevan's shores. Its relative height is about 450 meters, with a base diameter of around 2200 meters. In spring and summer, a small lake forms inside its crater, with a diameter of over 50 meters (Karakhanyan et al.,2004).

Volcano Eratumber, reaching an elevation of 2,485 meters, is part of a volcanic group encompassing fifteen volcanoes (Karakhanyan et al., 2004). Its craters exhibit closed ring shapes with steep walls of oxidized lavas and loose volcanic materials (Karapetyan et al., 1973). In contrast, Volcano Ajdaak, one of the largest peaks in the Gegham Highlands at 3,597 meters, displays a complex morphology (Aslanyan, 1958). It has a relative height of approximately 600 meters with a base diameter of around 3,000 meters. The central crater measures about 500 meters in diameter and reaches depths up to 70 meters. During the spring and summer, a crater lake forms within this crater, exceeding sixty meters in diameter (Karakhanyan et al., 2004). The slopes of Ajdaak feature lava flows intersected by erosional channels and areas of active geothermal activity.

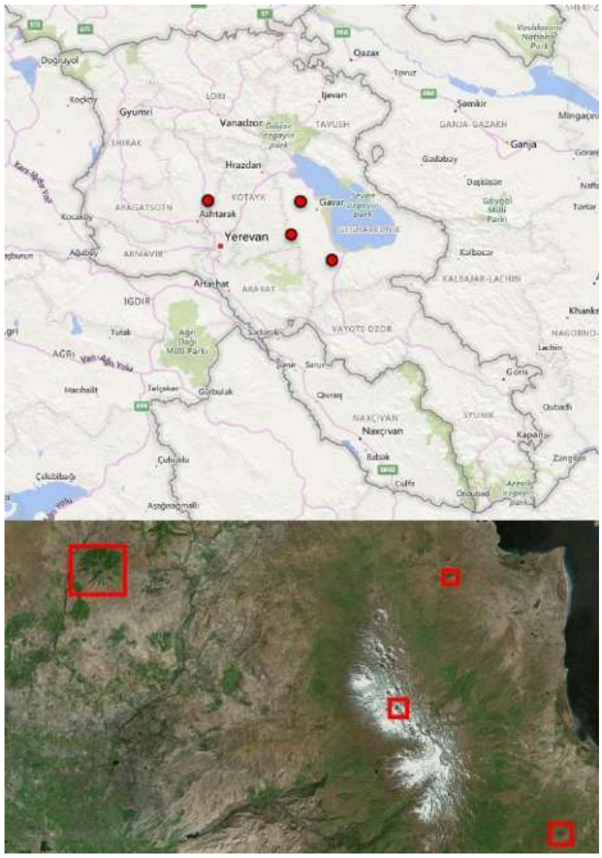

Figure 2. Study area.

2.2. Data and processing

The study of volcanic dome surfaces involves ground-based (field methods) and remote sensing methods (spectrometry, radiometry, altimetry, scatterometry, and radar and LiDAR). Each of these methods has its advantages and disadvantages. Combining both approaches ultimately yields the most accurate results because one method can offset the inaccuracies of another. In November 2023 and July 2024, two field trips were organized and successfully conducted to collect photographic and video materials necessary for subsequent mapping work. Ground verification is crucial for enhancing the accuracy and detail in cartographic data as it allows for direct inspection and evaluation of objects on-site (Casella et al., 2020).

During fieldwork, aerial photography was conducted using UAVs in optical, multispectral, and thermal ranges with the Mavic Pro, Mavic 3M (Multispectral), Mavic 3T (Thermal), and an RTK station to obtain coordinates with centimeter accuracy. Multispectral imaging was performed using the DJI Mavic 3M equipped with optical (4/3 CMOS, 20 MP) and multispectral cameras (G, R, RE, NIR, 5 MP) (Gewali et al., 2019). Thermal imaging was conducted with the Mavic 3T, which utilized optical and thermal cameras for a detailed analysis of volcanic rocks with different thermal conductivity. This allowed temperature anomalies related to volcanic activity and geothermal processes to be identified. For volcanoes, Arailer and Eratumber only optical imaging was performed; for volcanoes Armagan and Ajdaak, all three types of imaging were carried out.

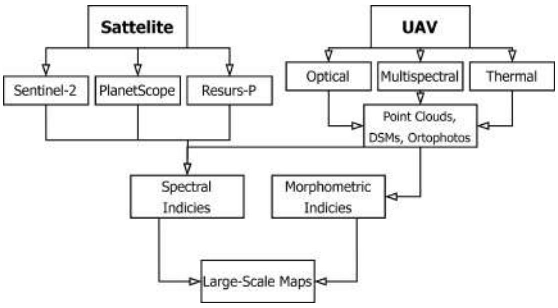

Figure 3. Data and processing steps.

Multispectral data from Sentinel-2, Resurs-P, and PlanetScope satellites were used to analyze volcanic structures across various spectral bands, including SWIR for volcanoes Armagan and Ajdaak.

Multi-temporal series of satellite images were obtained:

1. Sentinel-2
   a. Armagan: 240619, 240719, 240823, 240902, 240912, 241007
   b. Ajdaak: 240704, 230823, 240704, 240823, 240902, 240912
2. PlanetScope
   a. Armagan: 240620, 240706, 240711, 240821, 240827, 240929, 241006
   b. Ajdaak: 240704, 210810, 240823, 240829, 240903, 240904
3. Resurs-P
   a. Armagan: 240704

2.3. Processing and analysis

Photogrammetry is a method of obtaining metric and visual data about physical objects and landforms based on the analysis of multiple images (DeWitt et al., 2000). In this study, photogrammetric processing was applied to optical, multispectral, and thermal imagery from UAVs. Image processing was performed using Agisoft Metashape Professional software.

Photogrammetric processing involves several sequential steps aimed at obtaining highly accurate spatial data. Initially, images are imported; then they undergo quality filtering based on their quality and tilt angle (pitch): images with a quality below 80% or a pitch greater than 0.1° are removed, while those meeting the requirements proceed to the next stage. Subsequently, coordinate system reprojection is performed to align all images in a unified positioning system. To enhance image consistency, high-precision alignment is conducted. Next, a sparse point cloud reflects common points across images, followed by camera position optimization. In the subsequent step, a dense point cloud is built containing detailed spatial data, allowing a DSM to be created with moderate filtering. The final step involves forming an orthophoto — a detailed and geometrically correct representation of the studied area.

Digital product / Volcano	Tie Points	Dense point cloud	DSM	Orthophoto
Arailer	*843'986*	 *338'052'166*	 *46,3 cm*	 *23,16 cm*
Armagan	*748'314*	 *244'393'088*	 *15,2 cm*	 *7,6 cm*
Eratumber	*372'303*	 *150'988'995*	 *18,8 cm*	 *9,4 cm*
Ajdaak	*877'314*	 *90'982'028*	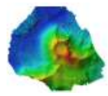 *25,6 cm*	 *12,8 cm*

Table 1. Digital products of photogrammetric processing.

2.3.1. Identification of morphometric features of the landforms

Various morphometric indices are used to identify landforms, calculated based on constructed digital surface models (DSMs). Morphometric analysis allows a more detailed study of relief features, soil formation, hydrological aspects, etc. Morphometric indices are numerical values that characterize the relief and enable the determination of erosion and prediction of hazardous slope processes. The morphometric analysis of relief was conducted using SAGA GIS software. For volcanoes Arailer, Armagan, and Eratumber, fourteen different rasters were created: analytical hillshading, slope gradient (slope), relative slope position (RSP), aspect orientation (aspect), plan curvature (plan curve.), profile curvature (profile curve.), convergence index (CI), closed depressions (CDs), total catchment area (TCA), topographic wetness index (TWI), LS-factor (LS-fact.), channel network base level (CNBL), channel network distance (CNDI), valley depth (VD). For the volcano Ajdaak, only slope gradient (slope), aspect orientation (aspect), and LS-Factor (LS-fact.) were analyzed.

2.3.2. Obtaining and analysing spectral indices

All data were combined into a single project to obtain detailed information about the surface of volcanoes Armagan and Ajdaak. Index images were constructed after loading satellite and aerial imagery from different dates. An optimal digital index was selected for each object being highlighted based on its distinguishability. For example, vegetation features are most clearly defined during the growing season; thus, analysis was conducted using July images. Meanwhile, soil characteristics are better distinguished outside the growing season; therefore, spring and autumn images were used for their study.

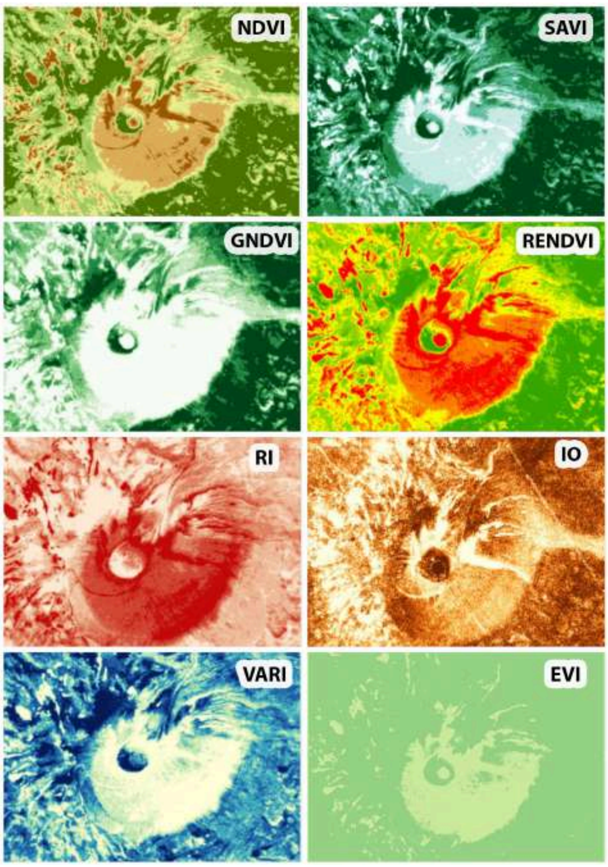

Figure 4. Spectral indices using the example of PlanetScope — Armagan — 240711.

NDVI, SAVI, GNDVI, and RENDVI indices were applied to highlight vegetation cover on land cover type maps. These indices allowed vegetation to be classified by density while considering various characteristics of vegetation and its relationship with soil conditions. For analyzing soil cover, the Iron Oxide Index, Redness Index, and Barren Soil Index were used to identify areas with red and black slag and determine zones with debris materials. Sentinel-2 PlanetScope and Resurs-P satellite data were applied for the overall segmentation of vegetation and soil, while Mavic 3M images were used to refine classification with high detail.

For highlighting vegetation cover on land cover type maps, the spectral indices were employed, allowing for detailed classification by density. The NDVI was used to determine the total area of vegetative cover and its density as it effectively distinguishes healthy from degrading or arid regions. The SAVI accounted for soil influence, which is crucial in areas with sparse vegetation near volcanic craters or slopes dominated by rocky debris. The GNDVI was utilized to assess plants' chlorophyll content, enabling differentiation between active versus suppressed vegetated zones. The RENDVI was applied to analyze the state of vegetative cover at different growth stages, allowing more accurate identification of high, medium, and low-density vegetated zones.

For analyzing soil cover, the Iron Oxide Index, Redness Index, and Barren Soil Index were used to highlight various geological formations on the map. The Iron Oxide Index (IO) was applied to identify areas with increased iron oxide content visible in sections with red volcanic slag. The Redness Index (RI) was used to assess the degree of soil saturation with iron compounds. This allowed for a more precise differentiation between areas with red slag and transitional zones where these materials mix with others. Additionally, aerial photography from UAVs enabled more accurate delineation of boundaries between different geological formations, including zones of red and black slag and areas of debris materials. The Barren Soil Index was applied to identify bare soil patches and rock outcrops that are useful for mapping debris material deposits. Data from Sentinel-2 PlanetScope and Resurs-P satellites were utilized for overall territory segmentation, allowing effective separation between vegetated and bare soil regions.

3. RESULTS

Thematic maps of the geomorphological structure and anthropogenic impact of volcanoes Arailer, Armagan, and Eratumber were compiled using visual interpretation methods and morphometric indices. For volcanoes, Armagan and Ajdaak maps were created using automated interpretation. Combining satellite and UAV data allowed for the detailed characteristics of volcanic domes to be obtained. Satellite data provided a wide spectral range and the ability to monitor changes over time, while UAV data offered high spatial resolution, enabling detailed analysis of individual areas.

The geomorphological map of volcano Arailer (1:15'000) details its main geomorphological features. The map displays the crater's primary and secondary cone rock walls formed by talus processes of plain surfaces and ancient lava flows that left marks on relief, as well as erosion canyons formed by water flow impact. Structures formed during lava cooling are also represented in detail within the crater. The cone's surface is covered with debris materials, indicating destruction processes. The "Anthropogenic Impact" map highlights forest shrub vegetation roads and agricultural lands, reflecting land use intensity. Detailed road networks are shown along with areas suitable for agriculture.

The geomorphological map of volcano Armagan (1:5'000) combines natural landforms and anthropogenic changes. It also features lava flows with hilly erosional microrelief, crater debris, material deposits, plain surfaces, and river valleys. Among anthropogenic objects, power transmission lines, roads, and tourist trails are highlighted. The presence of roads leading to a church and recreational areas confirms the territory's accessibility.

The map of volcano Eratumber (1:5'000) displays forms of relief and microrelief, including two secondary cones, one with a pronounced crater. The proximity of the river valley to the central cone is noted, which is essential for analyzing erosion processes. The eastern part of the territory is actively used in agriculture.

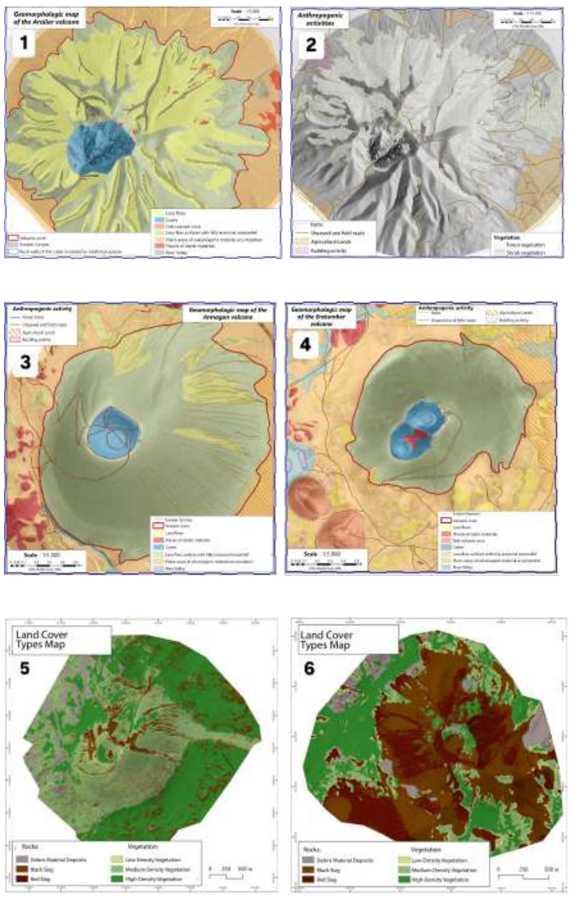

Figure 5. 1: geomorphological map of the Arailer volcano; 2: map of anthropogenic impact on the Arailer volcano; 3: geomorphological map of the Armagan volcano; 4: geomorphological map of the Eratumber volcano; 5: land cover type map of the Armagan volcano; 6: land cover type map of the Ajdaak volcano.

Based on the obtained images, automated interpretation was conducted for volcanoes Armagan and Ajdaak classes such as debris material deposits, black slag, red slag, low-density vegetation, medium-density vegetation, and high-density vegetation. Since volcano Armagan has a lower absolute height than Ajdaak, most of it is covered with vegetation, while Ajdaak has slopes without vegetation cover due to its height. Unlike the first part, where visual interpretation was performed, in this second part, fewer classes were identified. However, they more accurately demonstrate certain features that may not be noticeable to humans.

The central part of the volcano Armagan map is occupied by medium and high-density vegetation with a smooth transition between categories. The boundaries between vegetation and rocks are smoothed, which may indicate less detailed data processing. Since volcano Armagan has a lower absolute height than Ajdaak, the primary focus during its mapping was on differentiating types of vegetation, which was successful. Thanks to the separation of vegetation types, conclusions about slope processes occurring on the volcano (southeastern slope) can be drawn. The separation between vegetation and rocks was less successful; however, it allowed visual highlighting of roads on the slopes as they are not covered with vegetation. It was explicitly UAV data that enabled the distinction between vegetation and rocks, providing an opportunity to examine anthropogenic impact. Satellite imagery played a role in separating slag deposits and identifying debris material accumulations.

In the central part of Ajdaak's map, structures formed by slag and talus are visible. Boundaries between types of vegetation are clear, demonstrating high detail accuracy. Three types of vegetation have clear boundaries obtained through refinement using UAV data verified by field verification methods. Due to soil indices, black and red slags were also well-separated and visually checked against highly detailed orthophotos. High-resolution data allowed for apparent differentiation between vegetation cover and underlying surface without applying visual interpretation techniques for terrain analysis.

4. CONCLUSIONS

This study demonstrated the high effectiveness of integrating data from UAVs (optical, multispectral, and thermal imaging) with high-resolution satellite remote sensing data for large-scale thematic mapping of volcanic domes. The combination of UAV imagery and satellite data provided high spatial resolution and the ability to analyze various spectral indices, significantly improving mapping accuracy. The created cartographic materials allowed for a detailed assessment of the structure of the volcanoes in the Geghama Highlands.

The applied methods allowed the construction of spectral indices and the conduct of morphometric analysis. Integrating multiple data sources provided a comprehensive study of volcanic formations, significantly improving the accuracy of geological and geomorphological assessments.

Promising directions for further research include expanding the use of multispectral data and applying machine learning algorithms to improve the accuracy of relief classification. The introduction of remote sensing methods in combination with machine learning methods will allow for more accurate studies of the rock composition and vegetation cover of various geographic objects.

This study was fully supported by the Higher Education and Science Committee of the Ministry of Education, Science, Sport and Culture of RA in the frames of the research project No. IRF-22_04. Equipment support was provided by the Institute of Geography, Russian Academy of Sciences, State Assignment number FMWS-2024-0009 №1023032700199-9.

REFERENCES

Agisoft, 2023. *Agisoft Metashape Professional Edition*. Agisoft LLC.

Arutyunyan, E.V., et al. (2007). Geochronology of Neogene-Quaternary volcanism of the Geghama highland (Lesser Caucasus, Armenia). *Doklady Earth Sciences*, *416*(1), 1042.

Aslanyan, A.T. (1958). *Regional Geology of Armenia*. Yerevan: Publishing House of Yerevan University.

Asatryan, A. (1999). On the study of the flora and vegetation of Mount Arailer. *Proceedings of Young Researchers of NAS RA*, (1), 61-63.

Bannari, A., Morin, D., Bonn, F., & Huete, A. R. (1995). A review of vegetation indices. *Remote Sensing Reviews*, *13*(1-2), 95-120.

Bishop, M.P., et al. (2012). Geospatial technologies and digital geomorphological mapping: Concepts, issues and research. *Geomorphology*, *137*(1), 5-26.

Cameron, M., & Kumar, L. (2018). *Remote Sensing of Land Resources: Principles, Applications and Management*. CRC Press.

Casella, E., et al. (2020). Accuracy of sand beach topography surveying by drones and photogrammetry. *Geo-Marine Letters*, *40*, 255-268.

Choy, S., Bisnath, S., & Rizos, C. (2017). Uncovering common misconceptions in GNSS Precise Point Positioning and its future prospect. *GPS Solutions*, *21*, 13-22.

Coppola, D., Laiolo, M., Cigolini, C., Delle Donne, D., & Ripepe, M., 2016. Enhanced volcanic hot-spot detection using MODIS IR data: results from the MIROVA system. *Geological Society, London, Special Publications*, 426(1), 181-205.

DeWitt, B. A., & Wolf, P. R. (2000). *Elements of Photogrammetry (with Applications in GIS)*. McGraw-Hill Higher Education.

Durán, A. L., et al. (2020). Multi-method characterization of volcanic ash: a comprehensive approach. *Bulletin of Volcanology*, *82*(1), 1-23.

Favalli, M., Fornaciai, A., Mazzarini, F., Harris, A., Neri, M., Behncke, B., & Boschi, E., 2009. Evolution of an active lava flow field using a multitemporal LIDAR acquisition. *Journal of Geophysical Research: Solid Earth*, 114(B5).

Francis, P., & Oppenheimer, C. (2004). *Volcanoes*. Oxford University Press.

Förstner, W., & Wrobel, B. (2016). *Photogrammetric Computer Vision*. Springer Nature, Cham.

Gewali, S., et al. (2019). UAV-Based Remote Sensing for Precision Agriculture: A Review. *Remote Sensing*, *11*(22), 2737.

Harris, A. J. L., Flynn, L. P., & Rothery, D. A. (2005). *Remote Sensing of Volcanoes*. Geological Society.

James, M. R., Robson, S., & Eyjólfsson, G. Ö. (2017). Ultra-high resolution multi-temporal monitoring of volcano-ice interactions on Eyjafjallajökull, Iceland. *Journal of Volcanology and Geothermal Research*, *341*, 119-133.

Karapetyan, et al. (1973). *Geology of the Armenian SSR*. Yerevan: Publishing House of the Academy of Sciences of the Armenian SSR.

Karakhanyan, A., et al. (2004). Active volcanoes and volcanic hazard in the Armenian Highland and adjacent regions. *Proceedings of NAS RA, Geological Series*, *57*(1), 3-24.

Michalis, P., & Dowman, I. (2008). A Generic Model for Along-Track Stereo Sensors Using Rigorous Orbit Mechanics. *Photogrammetric Engineering & Remote Sensing*, *74*(3), 303-309.

Pinel, V., Poland, M. P., & Hooper, A., 2014. Volcanology: Lessons learned from synthetic aperture radar imagery. *Journal of Volcanology and Geothermal Research*, 289, 81-113.

Purnomo, N.H., et al. (2022). Geomorphological Mapping of The Prambanan Hills Yogyakarta. *MATEC Web of Conferences*, *372*, 05009.

Smith, J. (1987a). Close range photogrammetry for analyzing distressed trees. *Photogrammetria*, *42*(1), 47-56.

Smith, J. (1987b). Economic printing of color orthophotos. *Report KRL-01234, Kennedy Research Laboratories, Arlington, VA, USA.*

Smith, J. (2000). Remote sensing to predict volcano outbursts. *International Archives of Photogrammetry, Remote Sensing and Spatial Information Sciences*, *XXVII-B1*, 456-469.

Svyatlovsky, A.E. (1971). *Structural Volcanology*. Moscow: Nedra.

Svyatlovsky, A.E. (1982). *Morphometric Volcanology*. Moscow: Nedra.

Van der Meer, F. D., Van der Werff, H. M., Van Ruitenbeek, F. J., Hecker, C. A., Bakker, W. H., Noomen, M. F., & Woldai, T., 2014. Multi-and hyperspectral geologic remote sensing: A review. *International Journal of Applied Earth Observation and Geoinformation*, 14(1), 112-128.

Van Ruitenbeek, V., Cudahy, T., & Huntington, J. (2012). ASTER mineral mapping of the Goonumbla porphyry district, NSW, Australia. *Remote Sensing of Environment*, *119*, 174-188.

Westoby, M. J., Brasington, J., Glasser, N. F., Hambrey, M. J., & Reynolds, J. M. (2012). 'Structure-from-Motion' photogrammetry: A low-cost, effective tool for geoscience applications. *Geomorphology*, *179*, 300-314.